Effects of along-shore wind stress and surface cooling on the formation of shelf sea fronts in a simple air–sea interaction model

Lian Xie, Leonard J. Pietrafesa and Sethu Raman

Department of Marine, Earth and Atmospheric Sciences, Box 8208, North Carolina State University, Raleigh, NC 27695-8208, USA

Received 15 December 1995; revised 25 March 1996

This paper presents numerical simulation results from a set of control and sensitivity experiments on the effects of winter-time air–sea interaction on the variability of sea surface temperature (SST) on a two-dimensional continental shelf which is uniform in the along-shore direction and is bounded to the west by a straight coast and to the east by a prescribed Gulf Stream front. In the control experiment, the model ocean circulation is driven by a time-dependent wind forcing which is parameterically coupled to the cross-shelf SST gradient. In the sensitivity experiments, wind stress, diabatic cooling and air–sea coupling are turned on separately to estimate the individual contribution of each effect to the cross-shelf SST variation. Experiments have also been carried out for different coupling strengths and diabatic cooling rates to examine the model sensitivity to these parameters. The model results indicate that air–sea interaction could induce a secondary SST front on the shelf. Comparisons of model results with observations obtained during the Genesis of Atlantic Lows Experiment conducted off the east coasts of the Carolinas during January and February 1986 qualitatively confirm our finding.

1 Introduction

Sea surface temperature (SST) fronts or discontinuities of cross-shelf SST gradient often occur in coastal waters on the continental shelf margin off the southeast coast of the United States (known as the South Atlantic Bight, or SAB) during autumn and winter. These oceanic frontal structures can strongly influence both oceanographic and atmospheric processes in the SAB's environment. For example, SST fronts affect the coastal marine system by modifying cross-shelf transport of water masses [17], and influence coastal atmospheric frontogenesis [3,10,21], cyclogenesis [7,12], and low-level jetogenesis [8,23] by modifying the marine atmospheric boundary layer (MABL). Thus, modeling the formation and maintenance of SST fronts on the SAB shelf is extremely important for understanding coastal oceanic and atmospheric processes in that region.

SST frontogenesis on the SAB shelf has been simulated previously by Oey [16] using a two-dimensional, southeast coast ocean model uniform in the along-shore, meridional direction. He concluded that persistent northerly winds may promote SST frontogenesis on the SAB shelf in winter by driving upper Gulf Stream water onto the shelf. The mechanism is that the cross-shelf SST contrast is accentuated in the SAB region because the Gulf Stream provides a continual supply of warm water. Thus, even if offshore shelf and Gulf Stream waters were cooled by a loss of latent and sensible heat to the atmosphere, this loss is compensated for, in the stream proper, by more warm water advected from upstream. The result is that while shelf waters may cool to 5° to 10°C, waters just a few kilometers offshore in the Gulf Stream frontal region cool to only about 20°C. This differential cooling combined with onshore transport of upper Gulf Stream waters due to several days of southward winds would cause SST fronts on the middle shelf.

In the study of Oey [16], the interaction between the atmospheric flow and the SST front was not considered. However, observations and numerical simulations indicate that SST fronts on the shelf are conducive to the development of coastal mesoscale weather systems including fronts, cyclones and low-level jets [8,10,21]. Thus, when properly specifying the wind forcing for the ocean model, changes of wind conditions induced by SST should not be neglected.

In this study, we will apply a simple numerical model to investigate the impact of a time-dependent surface wind stress, which is parameterically coupled to the cross-shelf SST gradient, on the evolution of the cross-shelf SST distribution, over an idealized two-dimensional shelf. The text is organized as follows. In section 2, a simple two-dimensional model for SST frontogenesis on an idealized shelf will be described. Then, in section 3, we will present the results from a series of numerical simulations using the simple model. Qualitative comparisons of model results with observations are discussed in section 4 followed by a summary of conclusions in section 5.

2 Development of a simple two-dimensional model

We consider an initially uniform, motionless shelf water which is bounded to the west by a straight north–south coast and to the east by a sharp SST front (figure 1). The

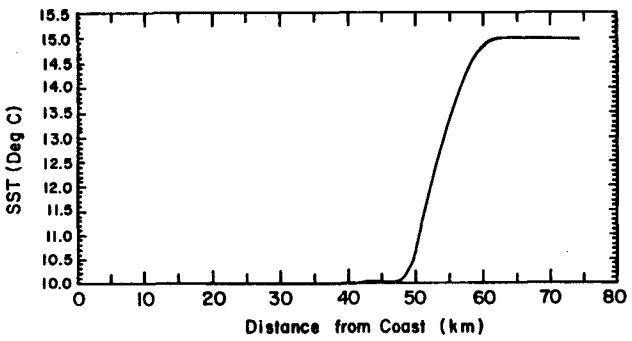

Figure 1. The initial SST distribution.

entire shelf is assumed to be 75 km wide. For convenience of discussion, the shelf is divided into three cross-shelf zones according to the distance from the coast: the inner (0–20 km), middle (20–45 km) and outer (> 45 km) shelves. The equations governing the changes of SST and surface currents will be presented below.

2.1 SST

The change of SST (T) is assumed to be caused by advection and diabatic cooling according to the following equation:

$$\partial T/\partial t + u\partial T/\partial x = -v\partial T/\partial y - w\partial T/\partial z - Q = Q_{net}, \tag{1}$$

where u, v, and w denote, respectively, the cross-shelf (x), along-shelf (y) and vertical (z) velocity components, Q represents the rate of diabatic surface cooling and Q_{net} is the rate of SST change due to the net effect of along-shore advection ($-v\partial T/\partial y$), upwelling ($-w\partial T/\partial z$) and diabatic cooling (Q). In a two-dimensional system uniform in the along-shore direction, the along-shore advection is zero, i.e.,

$$v\partial T/\partial y = 0,$$

and if the shelf waters are also well-mixed in the vertical (z), then,

$$w\partial T/\partial z = 0.$$

In this case, $\partial T/\partial t + u\partial T/\partial x = -Q = Q_{net}$. Mathematically, this results in a very simple equation for SST,

$$\partial T/\partial t = -u\partial T/\partial x - Q. \tag{1a}$$

The physical meaning of (1a) is that the local change of SST is caused by cross-shelf advection and diabatic cooling. These two effects are essential to frontogenesis in shelf waters as found by previous studies [2,16]. In addition, upwelling may be significant near the shelf break [11], and along-shore advection may be important near the coast and along the Gulf Stream [20]. To include the effects of upwelling and along-shore advection while still keeping a very simple equation for SST, we will use equation (1) and consider the effects of along-shore advection and upwelling as part of Q_{net} which is represented by a simple analytical function to be described below.

(i) Along-shore advection ($-v\partial T/\partial y$): Along-shore advection is important in the vicinity of the Gulf Stream. This results in very little change of SST in the along-stream direction near the Gulf Stream velocity core.

(ii) Upwelling ($-w\partial T/\partial z$): This term is usually small over the inner- and mid-shelves due to weak temperature stratification [1], but it may be important near the shelf break since both vertical velocity (w) and temperature stratification ($\partial T/\partial z$) are often significant there [11]. However, as pointed out by these authors, the magnitude of this term varies considerably depending on the location of the Gulf Stream.

(iii) Diabatic surface cooling (Q): This term is proportional to the air–sea temperature differential and surface wind speed. As pointed out by Riordan [21], Q is also proportional to the SST gradient in the direction of the airflow since surface air temperature is strongly influenced by SST along the upstream path of the airflow. As a result, during cold-air outbreaks when cold and dry northwesterly airflow moves offshore, maximum sea-to-air heat flux occurs near oceanic frontal features. Computations by Bane and Osgood [4] showed that during the second intensive observing period (IOP 2) of the Genesis of Atlantic Lows Experiment (GALE) conducted off the southeast U.S. coast in January 1986, the surface fluxes of both sensible and latent heat were largest over the Gulf Stream front. Their estimate showed that from January 25 to 30, 1986, the average heat loss to the atmosphere from the Gulf Stream mixed layer (where Q is expected to be a maximum) could have been sufficient to cool the Gulf Stream mixed-layer water by an average of 0.62°C. This is equivalent to a mean cooling rate of 0.1°C/day for the Gulf Stream mixed layer in the GALE study area.

Since both upwelling induced surface cooling and diabatic cooling increase from the shelf toward the shelf break (where the Gulf Stream front is often located), the combined effects of upwelling and diabatic cooling result in a maximum SST reduction near the shelf break. However, this reduction of SST is largely compensated for by the along-shore advection in the Gulf Stream proper. As a result, the net effect (Q_{net}) of upwelling, advection and diabatic cooling is a maximum SST reduction over the outer shelf.

To represent this combined effect of along-front advection, upwelling and diabatic cooling, we assume a Q_{net} of the form:

$$Q_{net} = \begin{cases} Q_0 \exp[(x - x_M)^2/25\ \text{km})^2] & \text{if } x > 25\ \text{km}, \\ Q_0 \exp[(25\ \text{km} - x_M)^2/(25\ \text{km})^2] & \text{if } x < 25\ \text{km}, \end{cases} \tag{2}$$

where $Q_0 = 0.5$°C/day, and $x_M = 50$ km representing the location of maximum SST reduction due to Q_{net}.

Equation (2) gives a qualitatively reasonable approximation of the SST cooling pattern across the SAB shelf, but, quantitatively, it is a simple estimate of the net effect of along-shore advection, upwelling and diabatic cooling. Our goal in this study is limited to a qualitative illustration of the air–sea interaction processes on the SAB shelf. For this limited goal, a more accurate quantitative estimate of Q_{net} is not warranted. Results from a more comprehensive model which does not involve the above approximation will be presented in a separate paper.

2.2 Cross-shelf current

In order to solve (1) for SST on the shelf, we need to estimate the cross-shelf surface current (u). Observations indicate that wind-driven subtidal frequency currents on continental shelves around the coastline of the continental U.S. display a near surface Ekman current response to local, along-shore wind forcing and opposite return flow near the bottom [5,11,13]. This is the so-called Ekman frictional equilibrium response (EFER). Conceptually, it is manifested over the southeast U.S. continental margin during southward along-shore winds as a cross-shelf onshore Ekman transport in a surface layer of thickness δ with an opposite (offshore) return flow in a bottom boundary of thickness layer δ_B. Based on the estimates of Pietrafesa [18], $\delta \sim 1.4 \times 10^{-4} v_a/f$, where v_a is the magnitude of the along-shore wind component and f is the local Coriolis frequency, and $d_B \sim 3.5 \times 10^{-5} v_a/f$. The offshore flow in layer d_B is induced by a barotropic, parabathic along-shore current which was estimated as $V_s \sim \tau^y/(\delta_B f \rho_w)$ or approximately $\sim 0.06 v_a$ and is geostrophically driven by a cross-shelf pressure gradient affected from a cross-shelf sea level slope [18].

The EFER of shelf circulation observed on the SAB shelf is analyzed by Xie and Raman [24] in a coupled low-order model. It was shown that a SST front near the shelf break can induce a northerly wind on the shelf. This northerly wind then drives a shoreward surface current and a seaward bottom current in the ocean. The surface-layer cross-shelf current (u) and the along-shore coastal current (v) are in general agreement with the solutions to wind-driven circulation on a well-mixed shelf [9]:

$$u = u_E[1 - \exp(-x/x_0)], \tag{3}$$

$$v = (\tau_y/H_E)\exp(-x/x_0)t, \tag{4}$$

where $u_E = \tau_y/(fH_E)$ is the Ekman drift velocity for waters sufficiently far away from the coast, H_E is the depth of the upper Ekman layer and τ_y is the southward wind stress. In this study, H_E is assumed as the upper boundary layer depth δ estimated by

$$H_E = \delta = 1.4 \times 10^{-4} v_a/f, \tag{5}$$

as proposed by Pietrafesa [18], and τ_y will be calculated according to the following quadratic stress law,

$$\tau_y = \rho' c_d |v_a| v_a, \tag{6}$$

where v_a is the surface wind speed, ρ' is the air-to-water density ratio and c_d is the drag coefficient. In all calculations, $\rho' c_d$ is taken as 1.7×10^{-6}.

Equation (3) shows that the u component of the wind-driven current is onshore under northerly winds. It decreases in magnitude toward the coast within a characteristic distance of x_0 from the coast, and approaches u_E when $x \gg x_0$. The v component is a geostrophic current caused by the diabathic pressure gradient set up via u_E driven by τ_y acting through the upper boundary (H_E). In the following calculation, we assume $x_0 = 20$ km, which is approximately the cross-shelf distance of the inner shelf. Within this region, surface wind stress drives a steady cross-shelf current and accelerates an along-shore geostrophic current (v). When bottom friction is considered, surface wind stress will ultimately be balanced by the friction and lead to a steady geostrophic along-shore current. Outside this region, the Ekman drift velocity u_E is the maximum cross-shelf surface current a constant wind would drive. Under our assumption, u_E represents the cross-shelf surface layer current over the middle and outer-shelf.

2.3 Surface wind

It has been suggested that SST fronts tend to form on the shelf off the southeast U.S. coast during persistent northerly, i.e. downwelling favorable winds in winter (e.g., [2,16,19]). Thus, a northerly ($\bar{v}_a$ or northeasterly basic wind is often used in numerical simulations of forced responses in the coastal sea–air system [10,22,26]. Xie and Raman [24] have pointed out that because of air–sea coupling, it is more realistic to also consider a mesoscale wind component (v_a') in addition to a uniform basic wind than considering the basic wind alone. This mesoscale wind component v_a' is significantly affected by the SST gradient on the shelf and thus may be parameterized by the latter. For example, assume v_a' as a function of the SST gradient. Such simple parameterization techniques have been widely used to parameterize the atmospheric response to SST anomalies [15]. Here, we will simply assume that the mesoscale component of the along-shelf wind speed (v_a') is a Gaussian function of the cross-shelf SST gradient:

$$v_a' = \alpha \, e^{-(\delta_x T - \delta_x T_{max})^2/\delta_T^2}, \tag{7}$$

where $\delta_x T_{max}$ is the maximum cross-shelf SST gradient on the shelf, δ_T is a constant which determines the cross-shelf length scale for v_a' (in the following calculations $\delta_T = 1°C/km$ is used). The value of α sets the upper limit of the perturbation wind speed induced by the cross-shelf

SST gradient. Observations and numerical experiments suggest that $\alpha \sim 10$ m/s [10,23].

Since v_a' is correlated to the SST gradient through (7), and the SST gradient is caused by v_a' through (1), (3) and (6), the atmosphere-ocean system described by (1)–(7) is a coupled system. However, since the dynamics of the atmosphere are not explicitly considered, the above system will be referred to as a parametrically-coupled system. To find a solution for this system, we start with a uniform northerly basic wind and assume the total along-shore wind speed (v_a) is the sum of the basic wind ($\bar{v}_a$) and the perturbation wind (v_a') which is initially zero and determined by (7) during the model integration. The surface wind stress is then computed from (6). After that, we allow this wind stress to act on the sea surface for 6 hours, and assume the surface current can be described by equation (3) with an air–sea coupling coefficient ϵ, i.e.,

$$u_{t_1} = \epsilon u_E [1 - \exp(-x/x_0)], \tag{8}$$

where $t_1 = 6$ hr, and $0 < \epsilon < 1$. After u_{t_1} is obtained, T_{t_1} can be solved from equation (1). We then compute δT at $T = t_1$ and calculate a new v_a' at $t = t_1$ from equation (7). Next, we hold v_a' constant in time for the next 6 hours, and repeat the above computation to get SST values at $t = 12$ hr, and so on.

The value of ϵ, which represents the ratio of actual surface drift velocity to the fully established Ekman drift speed, is difficult to determine precisely. In general, a larger ϵ value corresponds to a stronger coupling between the atmosphere and the ocean. Janowitz and Pietrafesa [11] showed that coastal sea level from Charleston, SC to Cape Hatteras, NC, the Carolina Capes region, is fully set up by the northerly, along-shore wind component within an 8–10 hour period over 2–10 day event time scales. Lee et al. [14] showed that the response time of wind driven surface currents is roughly 6 hours over the Georgia Bight mid-shelf and is less than 6 hours in the inner shelf and longer in the outer shelf. Thus over each 6 hr interval, the Ekman drift should be nearly established over the mid-shelf, but not yet established over the outer shelf. This implies that the value for ϵ is close to one over the mid-shelf but less than one over the outer shelf. For convenience, we choose a constant $\epsilon = 0.75$ for the entire shelf. The sensitivity of the model results to ϵ is discussed later.

3 Results

A total of eight experiments have been conducted. The input parameters of SST and surface wind for Experiments 1–6 as well as the purpose of each experiment are listed in table 1. The first (control) experiment is carried out with the set of model equations described in section 2 without further simplification. Experiments 2–6 are designed to estimate the respective contributions from basic wind, surface cooling and air–sea coupling to the

Table 1

Case #	Atmosphere	Ocean	Purpose
1	$v_a = \bar{v}_a + v_a'$, where v_a' is parameterically coupled to SST via equation (7)	Well-mixed shelf with a surface cooling specified by equation (2)	**Control experiment**: Examine the combined effects of surface cooling and Ekman transport induced by a parametrically coupled wind
2	Weak basic wind case: $v_a = -5$ m/s	Well-mixed shelf without diabatic cooling	**Sensitivity experiment**: Estimate SST variation caused by the Ekman drift induced by a weak basic wind.
3	Strong basic wind case: $v_a = -15$ m/s	No diabatic cooling as in Case 2	**Sensitivity experiment**: Estimate SST variation caused by the Ekman drift induced by a strong constant wind.
4	Parameterically coupled wind as in Case 1	No diabatic cooling as in Case 2	**Sensitivity experiment**: Examine the feedback effect of SST-induced mesoscale wind on SST
5	Weak basic wind as in Case 2	With diabatic cooling as in Case 2	**Sensitivity experiment**: Examine the combined effect of Ekman drift and surface cooling under a weak basic wind
6	Strong basic wind as in Case 3	With diabatic cooling as in Case 2	**Sensitivity experiment**: Examine the combined effect of Ekman drift and surface cooling under a strong basic wind

SST variation on the shelf. Finally, the sensitivity of the model to the coupling strength (ϵ) and diabatic cooling rate (Q_0) are examined in Experiments 7 and 8.

3.1 Control experiment

Consider first the combined effect of cross-shelf differential cooling and air–sea coupling. Equation (1) is integrated in time for three days with surface currents determined by equations (4)–(8). During the integration, air–sea coupling, which is described by equations (7) and (8), comes into effect every 6 hours. The simulated cross-shelf SST evolution is shown in figure 2a. It can be seen that the SST front, which is located near $x = 50$ km initially, progresses steadily shoreward and reaches $x = 37$ km at the end of Day 3. This leads to an increase of SST on the middle shelf between $x = 38$ km and 58 km as shown in figure 2b. Contemporaneously, waters shoreward of $x = 37$ km and seaward of $x = 58$ km are cooled as indicated by the decreases of SST in these two locations. It is worth noting that a secondary front, reflected by a kink in the SST curve near $x = 43$ km in figure 2a, formed on the middle shelf after Day 2. This is in agreement with the observed multiple frontal structures shown by Oey [16].

3.2 Sensitivity experiments

In order to understand the physical meaning of the model solution shown in figure 2, it is necessary to consider each and every effect involved in the model separately. In the following, the effect of basic wind, surface cooling and air–sea coupling will be discussed individually.

3.2.1 Basic wind

To isolate the effect of basic wind, we set the diabatic term Q to 0. In this slightly simplified problem, the local SST tendency is determined only by the cross-shelf advection of SST by the cross-shelf Ekman drift induced by a constant northerly wind. In this case, equation (1) becomes

$$\partial T/\partial t + u\partial T/\partial x = 0. \qquad (9)$$

Substituting equation (3) into equation (9) we can solve for SST (T). The solutions are illustrated in figures 3a and 3b corresponding to wind speeds of 5 m/s (Case 2) and 15 m/s (Case 3), respectively. Since no damping has been considered for either momentum or temperature, the initial (Gulf Stream) front has simply drifted shoreward "inviscidly". In the weak basic wind case, the

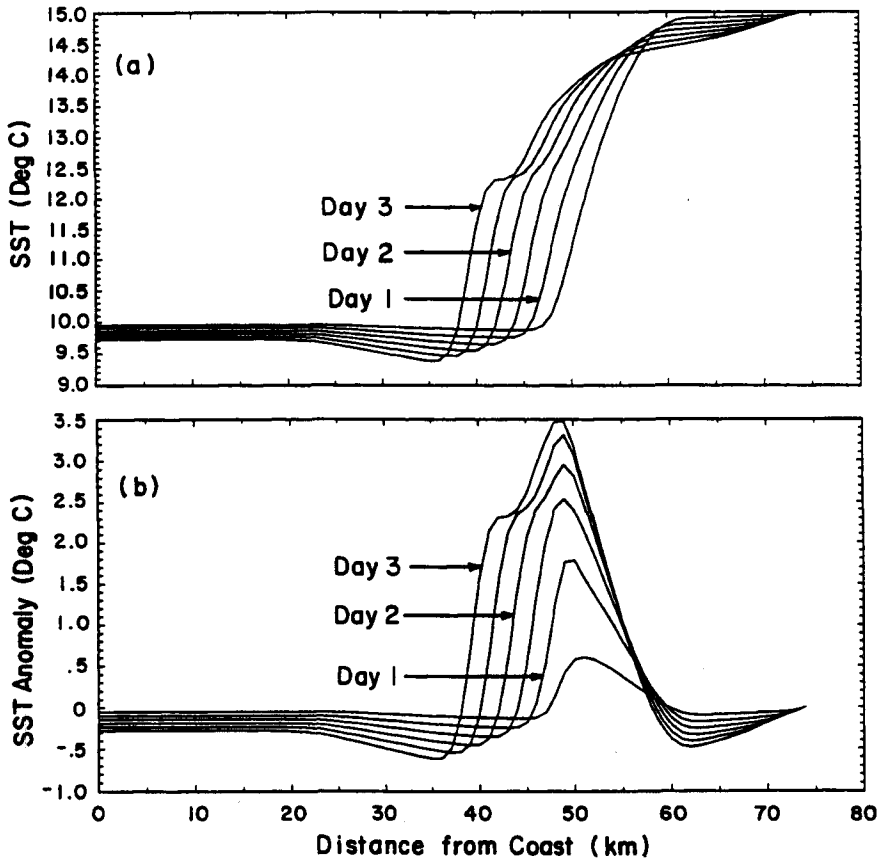

Figure 2. The evolutions of cross-shelf SST distribution and anomaly computed in the control experiment (Case 1): (a) SST; (b) SST anomaly.

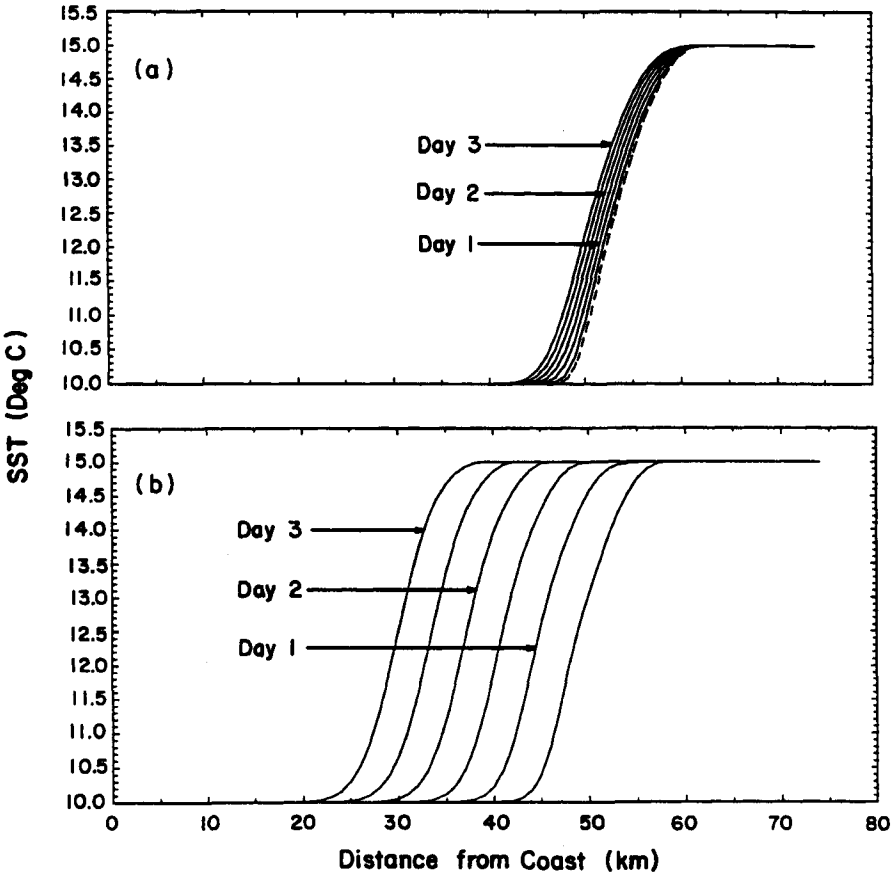

Figure 3. The evolutions of cross-shelf SST distribution induced by a uniform northerly wind: (a) $v_a = -5$ m/s (Case 2); (b) $v_a = -15$ m/s (Case 3).

Ekman drift velocity is on the order of 2 cm/s, or roughly 1.7 km/day. This gives an onshore penetration distance of less than 6 km by the end of Day 3. In the strong basic wind case, the initial frontal structure is advected rapidly toward the middle shelf at an average speed of roughly 11 cm/s or 9.4 km/day (figure 3b). In both cases, the cross-shelf temperature structure is almost unchanged by the end of Day 3. Thus, uniform basic wind alone does not induce any secondary frontal structure on the mid-shelf, at least in our simple model. So, what process has actually caused the secondary front in the control experiment (Case 1, figure 2)? Is it the air–sea coupling or the cross-shelf differential cooling? These questions will be addressed next.

3.2.2 Uniform wind and surface cooling

The experiments conducted in Cases 4 and 5 are, respectively, the same as that in Cases 2 and 3 except with a non-zero net cooling rate (Q_{net}) specified by equation (2). Figure 4a shows the evolution of the cross-shelf SST distribution in the case of weak basic wind (Case 4). Since the surface layer Ekman drift is very weak, the change in SST shown in figure 4a basically represents the net effect of surface cooling. This effect modulates the SST gradient near its initial location. Figure 4b shows the evolution of the cross-shelf SST distribution in the case of strong basic wind (Case 5). The difference between the weak and strong wind cases is that the former modifies the initial front near the shelf break since the front moves little over the period of model integration, but the latter modifies the front as it progresses shoreward. In both cases, the frontal structure resembles its initial shape except with some SST reduction both shoreward and seaward of the front. In either case, no secondary front formed on the middle shelf. This suggests that air–sea coupling, other than differential cooling, may be the cause of the secondary front formed in our control experiment. We will investigate this below.

3.2.3 Coupled wind without surface cooling

Here, we consider the effect of air–sea coupling in the absence of diabatic cooling (Case 6). The simulated evolution of cross-shelf SST distribution is shown in figure 5a, and the corresponding SST anomaly is shown in figure 5b. Clearly, a secondary front starts to form on the middle shelf near $x = 45$ km by the end of Day 2 and becomes evident by the end of Day 3 (figure 5a), similar to that shown in the control experiment (figure 2a). The corresponding mid-shelf warming shown in figure 5b also shows a secondary maximum on the mid-

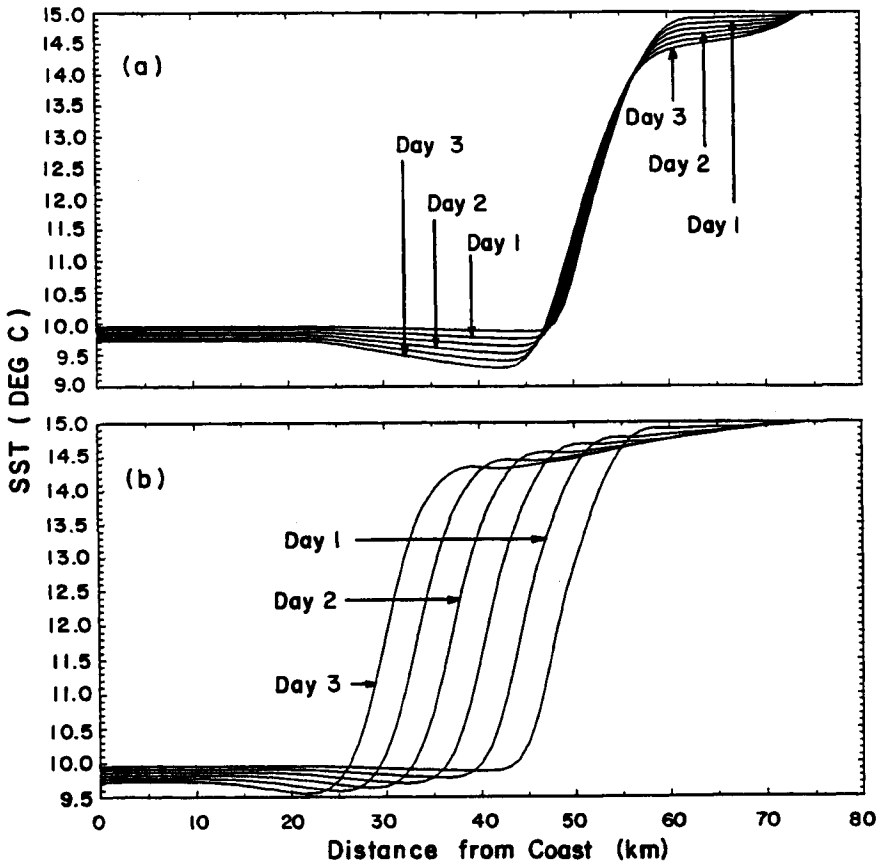

Figure 4. The evolutions of cross-shelf SST distribution induced by a uniform northerly wind and surface cooling: (a) for Case 4; (b) for Case 5.

shelf (between $x = 40$ and 45 km) on Day 3. Thus, the secondary temperature gradient on the middle shelf is apparently due to the correlation between the wind speed and the SST front. Therefore, air–sea coupling plays an important role in oceanic frontogenesis on the middle shelf.

3.2.4 Sensitivity to ϵ and Q_0

The air–sea coupling strength in our simple model is influenced by the choice of the two model parameters ϵ and Q_0. In Cases 7 and 8, a reduced surface cooling rate ($Q_0 = 0.25$°C/day), a reduced coupling coefficient ($\epsilon = 0.5$) and an increased coupling coefficient ($\epsilon = 1$) have been used, respectively. The resulting SST anomalies in each case are shown in figures 6a–c, respectively. The cross-shelf distributions of SST anomaly in figures 6a and c show a secondary maximum on the middle shelf similar to that seen in the control experiment, suggesting that reducing the cooling rate or increasing the coupling coefficient would still result in the formation of secondary frontal structures on the shelf. However, a reduced coupling coefficient has apparently smoothed out the secondary maximum of the SST anomaly. Therefore, cross-shelf SST distribution is sensitive to air–sea coupling, at least in our simple model.

4 Evidence of air–sea interaction during mid-shelf frontal genesis

Because mid-shelf fronts are mesoscale features with cross-shelf scales generally less than 20 km, high resolution observations of meteorological and oceanographic parameters are required to study air–sea interactions across a mid-shelf front. GALE experiment provided, for the first time, high-resolution observations of both meteorological and oceanographic data over the continental shelf off the southeast U.S. coast. For example, the temperature section (in °C) observed over the continental shelf region off Charleston, South Carolina on 24 January, 1986 shows a well-defined mid-shelf front at approximately 30 km offshore where the water depth is about 30 m (figure 7). Prior to the formation of this mid-shelf front (23–24 January), the along-shelf winds at inner and mid-shelf buoys deployed in the vicinity of the above-mentioned temperature section had shifted from northward to southward (figure 8a). Atkinson et al. [2] analyzed this case in detail and suggested that the transient northerly winds observed on the shelf were an important factor for the formation of the observed mid-shelf front. After the formation of the mid-shelf front, wind speeds over the inner and mid-shelf increased signifi-

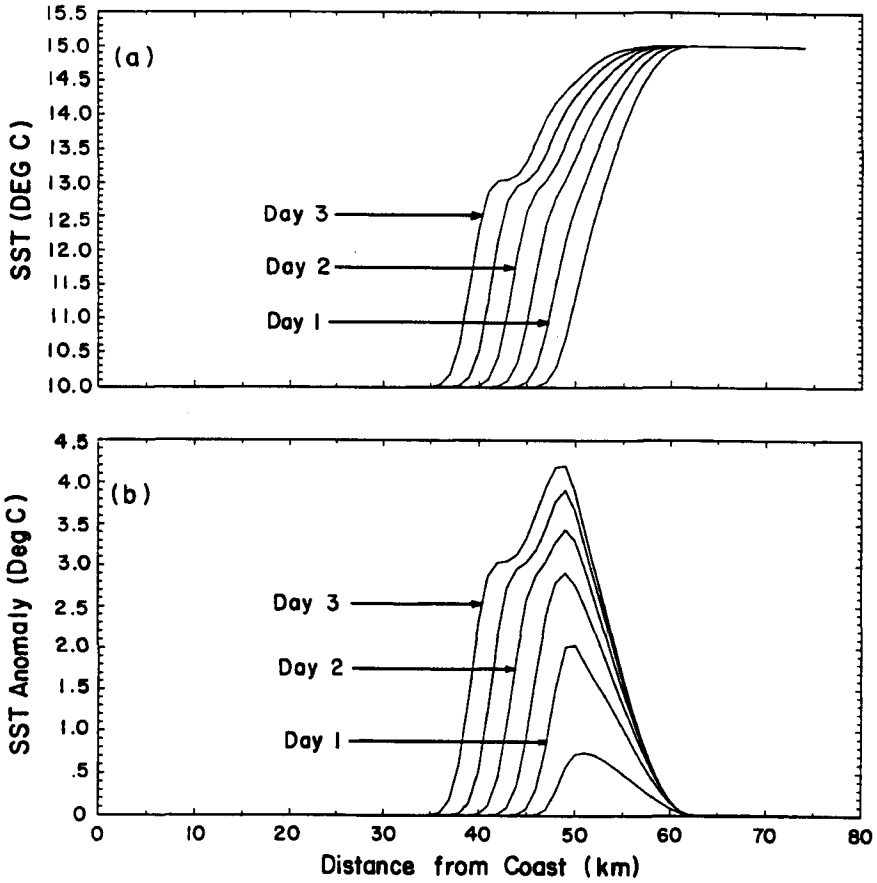

Figure 5. Same as figure 2 except no surface cooling (Case 6): (a) SST; (b) SST anomaly.

cantly (from about 5 m/s before 24 January to 12–15 m/s on 25 January). This suggests the existence of a feedback effect from the ocean to the atmosphere. Using the observed mid-shelf front on 24 January 1986 as a lower boundary forcing for a mesoscale atmospheric model, Huang and Raman [10] demonstrated that northerly surface winds could strengthen from approximately 7 m/s to 18 m/s in 6 hours (figure 8b). Therefore, on one hand, the atmospheric forcing played an important role in the formation of the mid-shelf front observed on 24 January 1986 as suggested by Atkinson et al. [2], and on the other hand, the mid-shelf front, in turn, caused a significant feedback effect on the surface wind field as shown by Huang and Raman [10]. This interaction between mid-shelf front and along-shore surface winds is consistent with our model result which indicates that air–sea coupling is important for mid-shelf frontogenesis off the East Coast of the Carolinas.

The simulated cross-shelf SST frontal structure which is characterized by a secondary front over the mid-shelf and a main front farther offshore (figure 2a) is also consistent with observations. Multiple, cross-shelf frontal structures on the Carolinas shelf similar to that shown in figure 2a have been reported previously by Oey [16]. Our data obtained on February 9, 1986 during GALE also shows a good agreement between the cross-shelf SST and along-shore wind distributions in the vicinity of an observed mid-shelf front. In this case, the National Center for Atmospheric Research research aircraft, King Air, had flown from A to C (figure 9a) to take wind and SST measurements. The wind speed measurements were taken at approximately 40 m altitude from A to C for a distance of 120 km at approximately 1620 UTC. The observed wind speed (southward) is plotted in figure 9b. The corresponding cross-shelf SST distribution is shown in figure 9c. A buoy data located near the coast (DUCK) is added to the section after adjusting the wind speed to the flight level. The wind section shows a speed increase from 3.5 m/s near the coast (DUCK) to approximately 6.5 m/s near point A, then to roughly 8 m/s 5 km east of A. It then increased gradually to 9 m/s near the Gulf Stream edge just west of B. When the aircraft crossed the Gulf Stream edge, the wind speed jumped up to 10.5 m/s. It then decreased rapidly on the eastern side of the Gulf Stream. The corresponding SST section shows that SST increased from approximately 5°C near the coast to a secondary maximum of 12°C at the mid-shelf (near A), and then decreased to a minimum of about 6°C before increasing sharply to more than 22°C at the edge of the Gulf Stream. Although it is not clear what caused the decrease of SST just west of the Gulf Stream edge, comparison of the SST section and

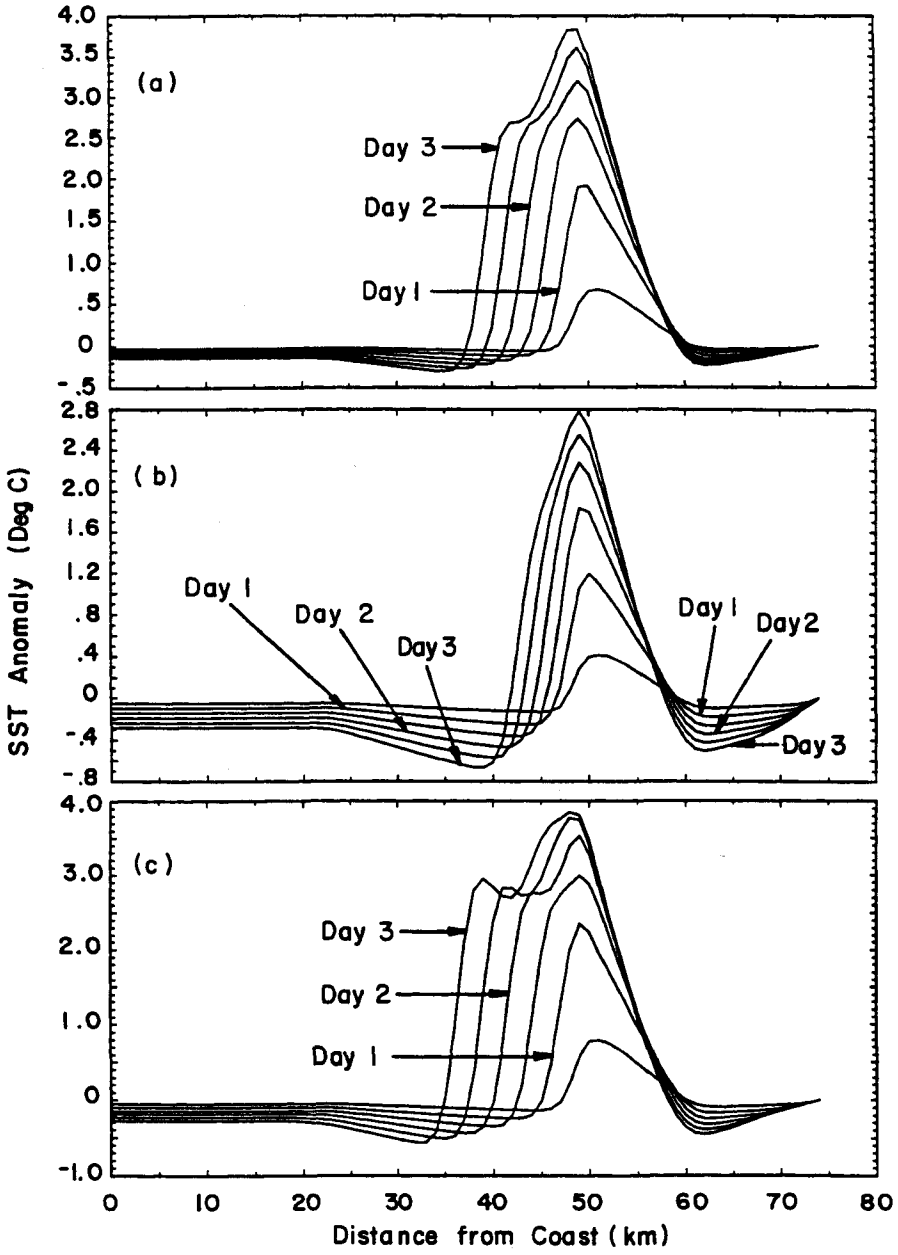

Figure 6. Sensitivity of model results to ϵ and Q_0. (a) $Q_0 = 0.25°C/day$; (b) $\epsilon = 0.5$; (c) $\epsilon = 1$.

the along-shore wind section clearly suggests a mid-shelf signature in both surface wind and SST fields. This indicates that the mid-shelf front and along-shore surface winds are perhaps coupled, as suggested by results from our simple model.

5 Conclusions

Results presented above indicate that a secondary SST frontal structure may form on the shelf through coupling of the along-shore wind stress and the cross-shelf SST gradient. A weak, uncoupled wind is, by itself, insufficient to cause ocean, mid-shelf front formation via surface Ekman drift. However, it should be cautioned that the calculations carried out in this study involve several simple parameterizations and the results are sensitive to the strength of the coupling. In a complementary study, we have found that mid-shelf frontogenesis can also involve forcing from bottom topography [26]. Thus, although simple models can help us to understand the basic physics associated with mid-shelf frontogenesis, realistic simulations of the mean and transient air–sea environments over the continental shelf require three-dimensional models with comprehensive physics and accurate initial and boundary conditions.

The intention of this study is to illustrate that air–sea interactions over a mid-continental shelf can signifi-

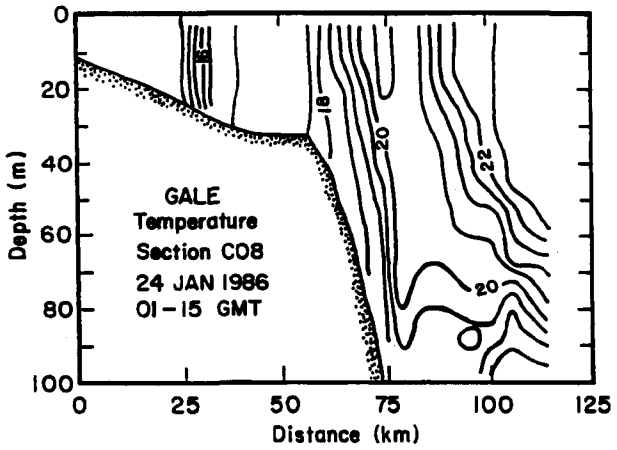

Figure 7. Observed temperature section on the shelf region off Charleston, South Carolina on 24 January 1986 (after Atkinson et al. [2]). It shows the existence of a mid-shelf front at 25–30 km off the coast.

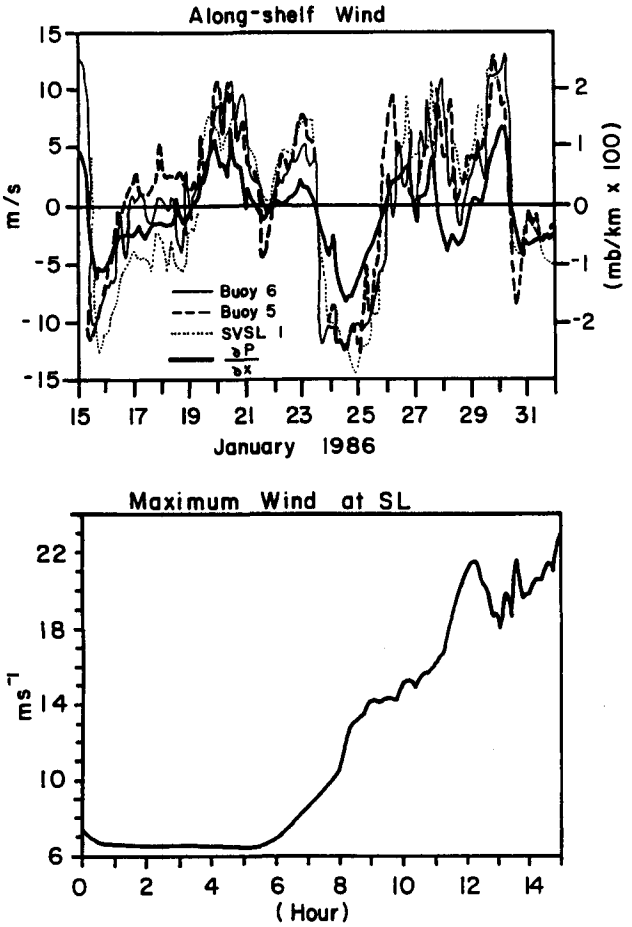

Figure 8. Surface wind speed over the continental shelf. (a) Along-shore wind speeds at buoy stations and cross-shelf pressure gradient in the GALE study area during January 15–31, 1986 (after Blanton et al. [6]). Buoy SVLS1 is located at 14 m depth (inner shelf) off Savannah, GA; Buoy 6 is at 26 m depth (mid-shelf) off Charleston, SC and Buoy 5 is at 32 m depth (mid-shelf) just north of Charleston. (b) Model simulated wind speed over the mid-shelf in response to the mid-shelf front during January 24–25, 1986 (after Huang and Raman [10]).

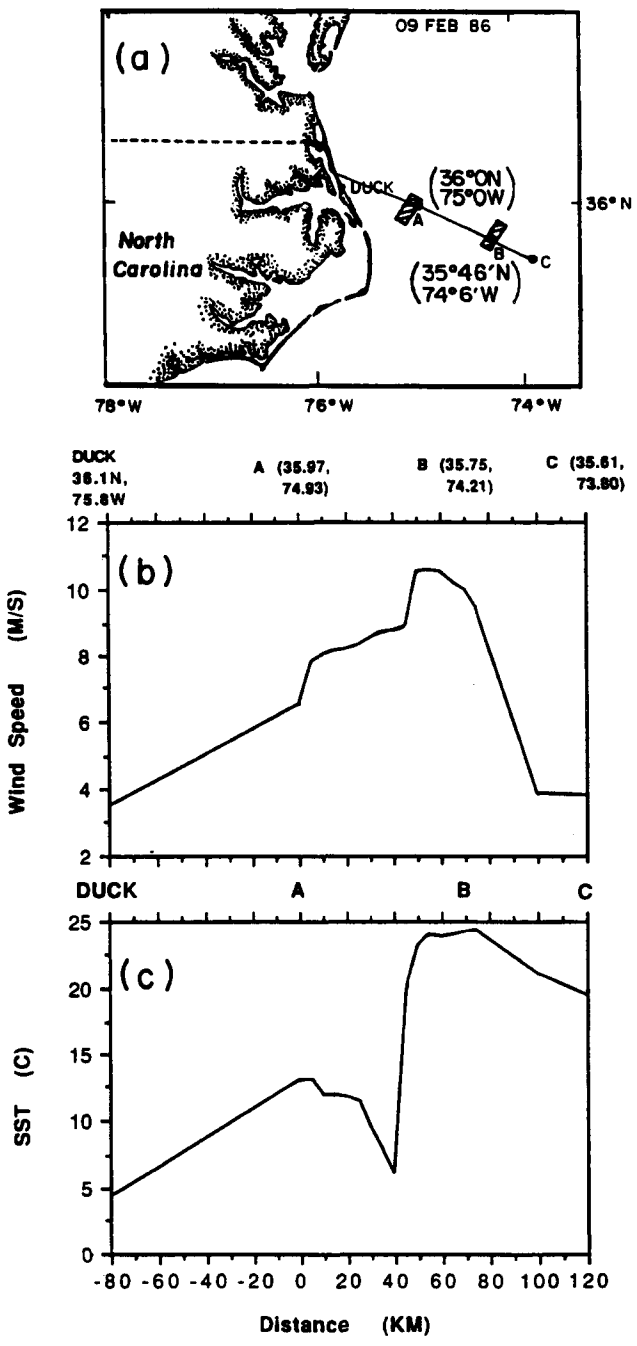

Figure 9. Cross-shelf distribution of along-shore wind speed and SST observed on 9 February, 1986. (a) Aircraft flight track during wind measurement; (b) observed wind speed at the flight level (40 m); and (c) observed SST.

cantly influence the structure of the cross-shelf SST distribution and may actually cause secondary SST fronts on the shelf. The concept of coastal air–sea interaction illustrated here using a simple model can be more convincingly studied using a three-dimensional coupled atmosphere-ocean model that is supported by well-designed field experiments. This will be the focus of future efforts.

Acknowledgements

The U.S. Department of Energy's Ocean Margin Program Grant #DEFG0985ER60376 (L.J. Pietrafesa), U.S. Department of Energy Atmospheric Radiation Measurements program under contract number 091575-A-Q1 with the Pacific Northwest Laboratories Atmospheric Sciences Division, and National Science Foundation Grant ATM9212636 (S. Raman), provided support for the study. L. Salzillo drafted the figures and M. DeFeo conducted the word processing.

References

[1] L.P. Atkinson, T.N. Lee, J.O. Blanton and W.S. Chandler, Climatology of the southeastern United States continental shelf waters, J.G.R. (Oceans) 88 (1983) 4705–4718.

[2] L.P. Atkinson, E. Oka, S.Y. Wu, T.J. Berger, J.O. Blanton and T.N. Lee, Hydrographic variability of Southeastern United States shelf and slope waters during the Genesis of Atlantic Lows Experiment: winter 1986, J.G.R. (Oceans) 94 (1989) 10699–10713.

[3] R.J. Ballentine, A numerical investigation of New England coastal frontogenesis, Mon. Wea. Rev. 108 (1980) 1479–1497.

[4] J.M. Bane and K.E. Osgood, Wintertime air–sea interaction processes across the Gulf Stream, J.G.R. (Oceans) 94 (1989) 10755–10772.

[5] R.C. Beardsley and C.D. Winant, On the mean circulation in the Mid-Atlantic Bight, J. Phys. Oceanogr. 9 (1979) 612–619.

[6] J.O. Blanton, J.A. Amft, D.K. Lee and A.J. Riordan, Wind stress and heat fluxes observed during Winter and Spring 1986, J. Geophys. Res. 94 (1989) 10686–10698.

[7] L.F. Bosart and S.C. Lin, A diagnostic study of the President's Day Storm of February 1979, Mon. Wea. Rev. 112 (1984) 2148–2177.

[8] J.D. Doyle and T.T. Warner, The impact of the sea surface temperature resolution on mesoscale coastal processes during GALE IOP 2, Mon. Wea. Rev. 121 (1993) 313–334.

[9] A.E. Gill, *Atmosphere-Ocean Dynamics*, Academic Press, New York, 1982.

[10] C.-Y. Huang and S. Raman, A three-dimensional numerical investigation of a Carolina coastal front and Gulf Stream rainband, J. Atmos. Sci 49 (1992) 560–584.

[11] G.S. Janowitz and L.J. Pietrafesa, A model and observations of time dependent upwelling over the mid-shelf and slope, J. Phys. Oceanogr. 10 (1980) 1574–1583.

[12] P.J. Kocin and L.W. Uccellini, A review of major East Coast snowstorms, Preprints, *10th Conference on Weather Forecasting and Analysis*, Amer. Meteor. Soc., Clearwater Beach, FL., 1984, pp. 189–198.

[13] T.N. Lee, W.J. Ho, V. Kourafalou and J.D. Wang, Circulation on the Southeast U.S. continental shelf, I, Subtidal response to wind and Gulf Stream forcing, J. Phys. Oceanogr. 14 (1984) 1001–1012.

[14] T.N. Lee, E. Williams, J. Wang, R. Evans and L. Atkinson, Response of South Carolina continental shelf waters to wind and Gulf Stream forcing during winter of 1986, J.G.R. (Oceans) 94 (1989) 10715–10754.

[15] J.P. McCreary, Jr. and D.L.T. Anderson, An overview of coupled ocean-atmosphere models of El Nino and Southern oscillation, J.G.R. (Oceans) 96 (1991) 3125–3150.

[16] L.-Y. Oey, The formation and maintenance of density fronts on U.S. southeastern continental shelf during winter, J. Phys. Oceanogr. 16 (1986) 1121–1135.

[17] L.J. Pietrafesa, G.S. Janowitz and P.A. Wittman, Physical oceanographic processes in the Carolina Capes, in: *Oceanography of the Southeastern U.S. Continental Shelf, Coastal and Estuarine Sciences*, vol. 2. American Geophysical Union, 1985, pp. 23–32.

[18] L.J. Pietrafesa, The Gulf Stream and wind events on the Carolina Capes shelf, NOAA-NURP (National Undersea Research Program) Research Report 89-2, 1989, pp. 89–129.

[19] L.J. Pietrafesa, G.S. Janowitz, K.S. Brown, F. Askari, C. Gabriel and L. Salzillo, The invasion of the Red Tide in North Carolina coastal waters, UNC SG-WP-88-1, 1988.

[20] L.J. Pietrafesa, J.M. Morrison, M. McCann, J. Churchill, E. Bohm and R. Houghton, Water mass linkages between the Middle and South Atlantic Bights, J. Deep Sea Res. II, 41 (1994) 365–389.

[21] A.J. Riordan, Examination of the mesoscale features of the GALE coastal front of 24–25 January 1986, Mon. Wea. Rev. 118 (1990) 258–282.

[22] A.J. Riordan and Y.-L. Lin, Mesoscale wind signatures along the Carolina Coast, Mon. Wea. Rev. 120 (1993) 2786–2797.

[23] L. Xie and Y.-L. Lin, Asymmetry of surface wind field forced by an elongated surface heat source, Preprints, *6th Conference on Mesoscale Processes*, Portland, Oregon, 1994.

[24] L. Xie and S. Raman, A simple nonlinear model for shelf air-sea interaction, Nonlinear World 1 (1994).

[25] L. Xie, L.J. Pietrafesa and S. Raman, Air-sea interaction over the continental shelf off the Carolina Capes, GOAS (1995), in press.

[26] L. Xie and L.J. Pietrafesa, Shoreward intrusion of upper-layer warm water by prescribed shelf-break temperature perturbation and surface wind stress, Geophysical Res. Letters 22 (1995) 2585–2588.